Two-dimensional fictitious truss method for estimation of out-of-plane strength of masonry walls

Muhammad Ridwan, M.D; Isamu Yoshitake; Ayman Y Nassif

Abstract: The truss method is rarely used to analyze a masonry wall, especially a masonry wall under a load in the out-of-plane direction. The present study proposes a model called the fictitious truss method (FTM) to determine the ability of masonry structures to withstand a lateral load within their elastic deformation capacities, and introduces a two-dimensional linear static model for masonry walls. The model represents the effect of flexural interaction by computing the stress and strain in the axial direction of the material and by considering uniaxial force effects on masonry elements. Pressure is applied to the surface area of the wall sequentially to predict the ultimate tension and compression cracking. FTM modeling is validated using previously obtained results for confined and unconfined masonry walls and for reinforced and unreinforced masonry walls. The FTM is a reliable method of assessing the out-of-plane strength of masonry structures owing to its conceptual accuracy, simplicity, and computational efficiency.

Keywords: fictitious truss method, masonry structure, out-of-plane strength.

Two-dimensional fictitious truss method for estimation of out-of-plane strength of masonry walls

Muhammad Ridwan[1] , Isamu Yoshitake[2] and Ayman Y. Nassif[3]

[1] Department of Civil Engineering, Padang Institute of Technology,
Jalan Gajah Mada Kandis Nanggalo Padang, Indonesia, e-mail: mhd.rid.wan.itp@gmail.com
(Ph.D. Candidate of Yamaguchi University) (Corresponding author)

[2] Department of Civil and Environmental Engineering, Yamaguchi University,
Tokiwadai 2-16-1, Ube, Yamaguchi, 755-8611, Japan, e-mail: yositake@yamaguchi-u.ac.jp

[3] School of Civil Engineering and Surveying, University of Portsmouth, Portsmouth PO1 3AH,
United Kingdom, e-mail: ayman.nassif@port.ac.uk

Abstract

The truss method is rarely used to analyze a masonry wall, especially a masonry wall under a load in the out-of-plane direction. The present study proposes a model called the fictitious truss method (FTM) to determine the ability of masonry structures to withstand a lateral load within their elastic deformation capacities, and introduces a two-dimensional linear static model for masonry walls. The model represents the effect of flexural interaction by computing the stress and strain in the axial direction of the material and by considering uniaxial force effects on masonry elements. Pressure is applied to the surface area of the wall sequentially to predict the ultimate tension and compression cracking. FTM modeling is validated using previously obtained results for confined and unconfined masonry walls and for reinforced and unreinforced masonry walls. The FTM is a reliable method of assessing the out-of-plane strength of masonry structures owing to its conceptual accuracy, simplicity, and computational efficiency.

Keywords: fictitious truss method, masonry structure, out-of-plane strength.

1. Introduction

The masonry wall is widely used for its low cost in low-rise construction in various countries. Additionally, a ring beam around a masonry structure (confined masonry) wall is recommended for the prevention of injuries and casualties that might occur in the unexpected collapse of a masonry wall. One form of masonry wall collapse is due to loading in the out-of-plane direction, which can occur, for example, in an earthquake or a flood. However, there is no indication that many masonry walls have collapsed under wind pressure after the completion of their construction [4], which can be considered evidence of the adequacy of their construction.

There is a connection between walls and reinforced concrete, given the different deformations of the two materials in response to loading. This is strongly dependent on the type of masonry used for infill. Masonry can be built using different kinds of units (e.g., solid or hollow), unit materials (e.g., clay or concrete), and mortar, depending on the region. The infill wall and the confinement are usually connected with mortar (unreinforced masonry) using an anchor and reinforcement (reinforced masonry).

Research on out-of-plane loading has included experiments and theoretical analysis using different analytical methods, but there has been far less research on out-of-plane loading of masonry walls than on in-plane loading of masonry walls. Some experimental studies have been performed on out-of-plane behavior of masonry reinforced walls [1–3], unreinforced masonry walls [4, 5], infill masonry walls [6–8] and confined masonry walls [9–11]. Based on these studies the main variables that affect the out-of-plane behavior of masonry walls are the aspect ratio (height divided by length), wall support conditions, wall slenderness ratio (height divided by thickness), axial load, in-plane stiffness of surrounding elements, wall openings, and unit type. Moreover, the out-of-plane behavior of confined walls is different than that observed for unreinforced, reinforced, and infill walls. The difference is mainly associated with construction procedures and wall reinforcement details. The differences between infill and confined walls are as follows. Firstly, confined walls consist of unreinforced panels surrounded by flexible reinforced concrete confining elements. The wall panels are constructed first, and later the confining elements are constructed. Infill walls consist of unreinforced or reinforced masonry walls surrounded by stiff concrete or structural steel frames [12]. The frames are constructed first, and later the masonry panels are constructed. This type of construction causes gaps between the frames and the masonry panels. Construction gaps delay the formation of arching action [6, 13].

The aspect ratio and slenderness ratio [4, 10, 12, 14] have been shown to affect the strength of unreinforced masonry (URM). Some researchers have used finite element (FE) theory and software to analyze masonry walls under out-of-plane loading. Drysdale *et al.* [4] used FE elastic plate analysis, Noor-E-Khuda *et al.* [1] used the explicit FE method and a layered shell model, and La-Mendola *et al*. [15] and Milani *et al*. [16] used commercial FE software. The FE method is very helpful, but it is complex and requires considerable cost.

On the other hand, numerical modeling of the out-of-plane response of infill frames was reviewed by Asteris *et al.* [17], whose in-depth literature review included some models of out-of-plane responses for infill frames. There are flexural-action-based models and arching-action-based models.

Cavalery *et al*. [18] investigated modeling of the out-of-plane behavior of masonry walls. They proposed analytical modeling of the moment curvature law and a numerical procedure to determine the flexural response of masonry cross sections, including nonlinearity owing to the σ–ε law in compression and the assumption of limit-tension material. This investigation simplifies the solution to a problem in which the bending moment increases because of increases in the eccentricity of the constant compressive axial load. This investigation used previous calcarenite and clay brick wall experimental data to validate the analytical model of the moment-curvature curve. This approach can be used for various classes of materials and structures, and is easy to apply means of the analytical moment-curvature law, allowing a fitted "exact" numerical result to be defined. In this investigation, the tensile strength was negligible."

Some researchers have also investigated near-surface-mount-reinforced masonry walls. [15, 19–22]. They used fiber-reinforced polymer (FRP), carbon-fiber-reinforced polymer (CFRP) strips, and polymer-textile-reinforced mortar to reinforce a masonry wall. These materials are used to improve the out-of-plane performance of a URM wall. Near-surface-mount-reinforced masonry walls are very helpful in increasing the strength of masonry but are strongly affected by the type of reinforcement used.

URM panels in reinforced concrete frames were investigated by Tu *et al.* [8] and Furtado *et al.* [23]. Tu *et al.* investigated the out-of-plane behavior of URM walls in shaking table tests. They used an analytical model for analysis. Furtado *et al.* evaluated the combination of in-plane and out-of-plane behaviors by comparing two infill masonry walls subjected to monotonic out-of-plane loading and cyclic out-of-plane loading.

Many theories have been proposed to investigate the strength and behavior of masonry structures in the out-of-plane direction, as shown in **Table 1**. However, these theories are based on and limited to certain experimental configurations. Most studies on the out-of-plane behavior of masonry walls have been experimental works and thus time-consuming and expensive [1]. It has been concluded that the method that most accurately predicts the out-of-plane strength of confined walls is the bidirectional strut method. This method is an iterative procedure based on two-way arching action.

The truss model is rarely used in calculations for a masonry wall structures, but several truss models have been extensively used for analysis of the nonlinear behavior of masonry infills. A truss model for masonry structures was proposed by Lu *et al*. [24] in research on a nonplanar reinforced concrete wall. Recently, Moharrami *et al*. [25] used the truss model for the analysis of masonry structures employing nonlinear truss modeling, which was used in the analysis of shear failure in the in-plane direction of the wall.

The present study proposes a new method of using a truss as a structural element of a masonry wall in order to analyze the out-of-plane strength of a masonry structure. The aim of present study is a model oriented to the determination of out of-plane resistance. The proposed fictitious truss method (FTM) provides practitioners and academics with analytical results and can be modified for a variety of masonry walls.

2. Material and Methods

The FTM creates patterns of stress distribution in a flexural element structure. The geometry of the FTM is obtained by centralizing and simplifying the force acting on a wall. The elements establish truss blocks and then configure the truss structure as indicated in **Fig. 1.**

2.1 Determination of truss geometry

A truss model requires cross-sectional dimensions and determination of the geometry of truss elements as well as applicable material models. The first step is establishing the dimensions of the truss and of the truss elements considering the real dimensions of the masonry structure. In the cross section of the masonry structure, ***t*** is the thickness of the masonry and is not directly used in the FTM models.

The FTM makes the following assumptions. The thickness of the masonry wall is the initial height of the truss model (t). The effective cross section of the truss element is a square shape (a x b_{eff}.), the cross section is the effective area of compression stress in a flexural beam, the aspect ratio is less than one (i.e., H/L < 1), and the truss is fictitious. The truss can be calculated as a numerical value until early fracture, and buckling can be ignored. If reinforcement is used, its arrangement must be regular.

The shape of the truss model is shown in **Fig. 2**. There are three types of shapes: v_t is a vertical truss, h_t is a horizontal truss, and d_t is a diagonal truss. A diagonal truss can be a single diagonal or double diagonal truss.

The truss geometry defines the geometry of the vertical cross section of the brick and determines the height of the masonry wall. Each block truss is the representative geometry of the brick and mortar. The height of the truss (v_t) is the effective width of a cross section of the masonry wall (t_{eff}), while the width (h_t) of the truss is the effective thickness of the mortar or unit masonry. b_{eff} is the assumed width of the unit load to be used. It is obtained from the length of the brick unit. t_{eff} is the effective height of a cross section of the truss model. It is obtained from the equivalent inertia of the effective cross section as shown in **Fig. 3** and by solving equation (1) below:

$$I_{tot} = I_{eq}, \tag{1}$$

where $I_{tot} = \frac{1}{12} b_{eff} t^3$ and I_{eq} is the inertia unit equivalent of the masonry element which can be solved with the provision that A_1=A_2 and the equation

$$I_{eq} = \sum_1^n I_n + \sum_1^n (A_n y_n^2) \tag{2}$$

y is thus obtained if n = 2 as

$$y = \sqrt{\frac{I_{tot} - 2I_n}{2A_n}}. \quad (3)$$

The result is that t_{eff} is $2y$

The total height of the vertical truss elements is $t_w = 2y + a$; however, the height used in the analysis (t_{eff}) is $2y$ as indicated in **Fig. 4**. **Figure 3** shows the determination of the effective height of a truss element that has parameters for the equivalent stress of the block parameter.

The total stress area in compression is $A_c = a\, b_{eff}$. In accordance with SNI 03-2847-2013 [31], the depth of the equivalent stress block (a) is obtained as $a = \beta_1 c$, where c is the distance from the center of mass to the top and $\beta_1 = 0.85$. β_1 is a function of the strength class of materials: $\beta_1 = 0.85$ for $f'_{me} < 30$ MPa, and is reduced by 0.008 for every increase of 1 MPa in compressive strength; it should not be less than 0.65. Therefore, $a = 0.85c$ and $\alpha = 1$ for actual compressive strength, and 0.85 for the compressive strength equivalent. b_{eff} is the length of the brick or the length of the effective area of pressure used as the effective width. $A_c = A_t = a\, b_{eff}$ is used for a masonry wall without reinforcement and $A_t = A_r$ is used for a masonry wall with reinforcement, where A_t is the area of tension, A_c is the area of compression, and A_r is the area of reinforcement. Typical cross-sectional dimensions used in the FTM are shown in **Fig. 1.**

The geometric dimension of the mortar part is the same for the brick and unit parts. The material parameters should be set according to the properties of each material, and the material modeling assumption in tension and compression is isotropic, linear, elastic material. An elastic material may show linear or nonlinear behavior. In this study, we assume linear behavior. For linear elastic materials, stresses are linearly proportional to strains ($\sigma = E\varepsilon$) as described by Hooke's law. The law is applicable for material properties that are independent of coordinates (homogeneous) and material properties that are independent of the rotation of the axes at any point in a body or structure (isotropic materials). Here only two elastic constants (modulus of elasticity E and Poisson's ratio ν) are needed for linear elastic materials.

The FTM can be used to determine the strength of a confined or unconfined masonry structure in the out-of-plane direction.

2.2 Schematic of the FTM

The FTM determines the out-of-plane strength of a masonry wall structure and involves the following steps:

- Check that the aspect ratio (H/L) of the masonry structure is less than 1.0.
- Provide material properties including the elasticity, specific gravity, Poisson's ratio, compressive strength, tensile strength, and others.
- Determine the widely assumed pressure area (b_{eff}).
- Determine the effective height of the element truss ($a = \beta_1 c$).
- Arrange $A_c = A_t = a\, b_{eff}$ to obtain y (**Eqs. 1, 2, 3**).
- Determine the effective thickness of the truss structure $t_{eff} = 2y$.
- Obtain the model and its dimensions by determining the boundary conditions of the masonry structure.
- Analyze the FTM structure to obtain the element truss force.
- Apply the load (P_{eq}) gradually until there is cracking in areas of tension and compression.

All loads are applied as concentrated equivalent loads acting on the truss joints. The FTM is schematically shown in **Fig. 5.**

The FTM may not be applicable physically, but it can be performed numerically. The element truss force can be analyzed using classical mechanics methods, other methods typically used to calculate truss structures, or using FE software. After determining the truss element and truss structure, the loading can be applied gradually while checking the strain in compression and the tension truss element condition.

2.3 Material models

The stress–strain relationship of truss elements representing masonry walls is shown in **Fig. 6.** The tensile strength and compressive strength of the mortar and the units are interconnected. In the present study, the vertical and horizontal truss elements are the studied variables while the diagonal truss element distributes forces to the vertical and horizontal truss elements.

The material model of masonry is linear and elastic for brittle material; likewise for units and mortar. The failure criterion of the FTM model is the maximum principal strain by uniaxial loading on a truss member. The Hooke's law concept $\varepsilon = \frac{\sigma}{E}$ can be applied to predict when either of the principal strains resulting from the principal stresses ($\sigma_{1,2}$) meets or exceeds the maximum strain corresponding to the yield strength (σ_y) of the material in uniaxial tension or compression.

The FTM requires the force acting on a truss element to be in the critical region of the mid-span of the truss structure, where there is tension and compression on either side. Tension and compression may occur in mortar and brick in structural elements. It is therefore necessary to choose either brick or mortar as the material when determining the strength of masonry structures.

Almeida *et al*. [26] investigated hollow bricks and the brick–mortar interfaces under uniaxial tension for hollow bricks sourced from Portugal and Spain. Testing various brick types revealed a similar uniaxial response in tension and compression (**Fig. 6**). **Figure 6a** shows the relationship between tension stress and strain. Stress increases linearly to a peak value before gradually and nonlinearly decreasing. The present paper focuses only on the behavior until the peak tensile load is reached. The same behavior is seen for both raw materials and materials such as FRP, CFRP, and steel. Almeida *et al*. [26] found that elongation values for hollow brick obtained with different peak tensile loads ranged from 3 to 10 μ while those for mortar were less than 5 μ. The tensile stress values ranged over 2.75–3.82 and 1.93–2.25 N/mm^2, respectively, for the hollow brick and mortar. In the present study, the tensile stress was assumed to be 3 and 2 N/mm^2, respectively, for the hollow brick and mortar, and the tensile strain was assumed to be 0.001. **Figure 6b** shows the relationship between compression stress and strain.

Kaushik *et al.* [27] found cracking at strain values from 0.0023 to 0.00375. Based on these data, the present study used 0.003 as the cracking point for masonry elements. Kaushik *et al.* stated that the values of E_b, E_j, and E_m for masonry walls are approximately

$$E_b \approx 300\, f_b, \tag{4}$$

$$E_j \approx 200\, f_j, \tag{5}$$

$$E_m = 550\, f'_m. \tag{6}$$

Corresponding coefficients of variance were 0.35, 0.32, and 0.3 respectively. These results are in line with the basic formula used by Eurocode 6 [28] regarding the characteristic compressive strength of masonry. Following the above research, E_b, E_j, and E_m for masonry can be used in the present study; however, the present study considers the elastic linear range.

2.4 Aspect ratio, slenderness ratio, and weight reduction

A masonry structure comprising multiple walls subjected to out-of-plane loading has an aspect ratio (*AR*). The present study does not consider $AR \geq 1$ except for the case of the one-way vertical wall (with a plane of failure parallel to the bed joints). This is because several previous studies [14] revealed that structural rigidity is higher in the horizontal direction than in the vertical direction if $AR \geq 1$. However, the approach of using $P = (0.3AR + 0.7)\ P$ can be invoked for AR> 1.

The slenderness ratio also affects the masonry structure. The thickness of a masonry wall (t) affects the stiffness and strength of the wall. In the present study, t is a variable that has been resolved in various stages used in determining the stiffness and strength of a masonry wall. The stages seek the equivalent thickness of the wall (t_{eff}), which represents the truss.

In structural analysis using, for example, FE software, self-weight is calculated automatically. A solid element is used as the truss element. Therefore, the specific gravity of the truss must be adapted to the specific gravity of the solid masonry elements. This can be achieved by multiplying the specific gravity by a factor ξ for masonry elements:

$$\gamma_{eq(u)} = \xi\gamma_u \tag{7}$$

$$\gamma_{eq(m)} = \xi\gamma_m \tag{8}$$

where $\xi = \frac{b_{eff}\ t}{2a\left(\frac{t_{eff}}{\sin\theta}+t_{eff}+b_{eff}\right)}$, γ_{eq} is the specific gravity equivalent of a unit or of mortar, ξ is the specific gravity factor, γ_u is the specific gravity of the unit, and γ_m is the specific gravity of the mortar. Geometrically, the self-weight of a truss element affects the behavior of masonry structures. The load given to the structure is therefore an additional external load. For instance, if the thickness of the wall is (t) = 120 mm, the width of the unit load to be used is (b_{eff}) = 210 mm, the depth of the equivalent stress block is (a) = 51 mm, and the effective width of a cross section of the truss model is (t_{eff}) = 69.13 mm, then the value of the specific gravity factor (ξ) is 0.655. This value has a significant influence on the self-weight of a masonry structure.

3. Results

The FTM was validated using the results of analysis of out-of-plane masonry structures conducted in previous studies. Truss analysis can be performed by using matrix methods as for a two-dimensional truss using the direct stiffness method. In this study, this is performed using SAP2000 software [31]. The basic data are entered in accordance with the constitutive modeling approach. Both truss shapes were used and validated for masonry wall structures subject to out-of-plane loading. Material properties from the literature were used as input data in analyzing the FTM structure with FE software.

3.1 Validation 1

The first validation of the FTM was conducted for a model used by Varela-Rivera *et al.* [9], namely six confined masonry walls with reinforced concrete. The specifications of the materials and dimensions of the walls are given in **Table 2**. Each wall was comprised of hollow blocks in a half-running bond pattern. The dimensions of the concrete confining elements were 0.15 x 0.2 m × 0.4 m for E-1, E-2, E-4, and E-5, and 0.12 m × 0.2 m × 0.4 m for E-3 and E-6. Each wall was confined by reinforced concrete around its perimeter. A load was applied to the masonry wall using air bags with dimensions of 1.2 m × 3 m (**Fig. 7**).

The air bags were filled gradually until the ultimate cracking of the masonry walls. The thickness of mortar connecting the blocks of masonry units was 10 mm.

The results of this numerical experiment (W_e) were compared with those obtained by Varela *et al*. [10, 11] using the spring–strut method (W_{ss}), and were previously compared with the results of previous studies conducted by Varela-Rivera *et al.* [9] using the yield-line method (W_{yl}), failure-line method (W_{fl}), and compressive strut method (W_{cs}). The yield-line method (W_{yl}) is theoretically not recommended for brittle materials such as masonry, but is still used to predict the out-of-plane strength of walls [4]. The failure-line method (W_{fl}) is a modification of the yield line method based on the idea that, prior to the formation of the final failure cracking pattern, some cracks are already formed, and their contribution to the internal work should not be included. For this reason, the failure line method predicts lower strength than the yield line method. The compressive strut method (W_{cs}) was proposed by Abrams *et al*. [6] for infill walls surrounded by concrete frames. In Abrams' work, an infill wall was subjected to uniform pressures. It was assumed that, after the formation of a given cracking pattern, a wall was divided into segments.

The structure and description of the walls and the FTM model proposed here are presented in **Fig. 8.** Results of FTM analysis are denoted by W_t and W_c. FTM results are presented and incorporated in **Fig. 9**.

The example calculations of b_{eff} and t_{eff} are as follows:

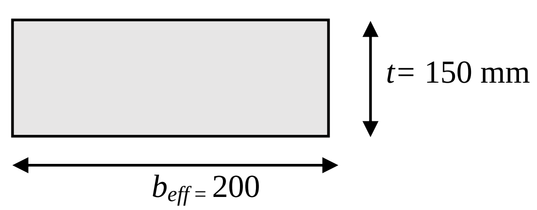

$$I_{tot} = \frac{1}{12} b_{eff} t^2 = 56{,}250{,}000 \text{ mm}^4$$

$c = 0.5\,t$, β=0.85 $\rightarrow$ a = cβ =75 x 0.85 = 63.75 mm

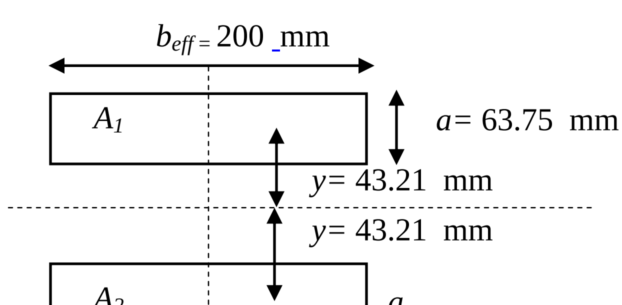

$$I_{eq} = \sum I_n + \sum A_n y^2$$

I_{eq} = 56,250,000 = I_{tot}

n	I_n =1/12b_{eff}.a^3 (mm^4)	A_n = b_{eff}.a (mm^2)	y^2	(mm^4)
1	4,318,066.406	12,750	1,867.21	28,125,000
2	4,318,066.406	12,750	1,867.21	28,125,000
Σ	8,636,132.813		I_{eq} =	56,250,000

y is calculated by using the "goal seek" command in Microsoft Excel software or by Equation 3:

$$y = \sqrt{\frac{I_{tot} - 2I_n}{2A_n}} = 43.21 \text{ mm}$$

The result is that y = 43.21 mm; hereafter, t_{eff} = 2y = 86.42 mm and t_w = 150.17 mm.

FTM results are explained further in the Discussion section.

3.2 Validation 2

The second validation of the FTM was conducted for a model used by Hamoush *et al.* [29], who investigated the behavior of a surface-reinforced masonry wall under out-of-plane loading. The wall was reinforced with FRP and had dimensions of 900 mm × 600 mm × 200 mm. There were 18 specimens in total. Specimens had a single or double layer of FRP and a distance from the fiber to the support of 0, d/2, or d/4, where d is the span from the support to the first of point load on the masonry wall specimen. Specimens were constructed with hollow bricks made from mortar with a thickness of 25 mm. A single hollow block unit had two holes. The dimensions of a hollow block were 400 mm × 200 mm × 200 mm. The thickness of the HB was the effective compressed zone in this validation. The web fiber used in the validation was constructed with Tyfo Hi-Clear epoxy resin with an ultimate tensile strength of 414 MPa, ultimate elongation of 2.0%, elastic modulus of 27,580 MPa, and design thickness of 0.4 mm per layer. The Hamoush test setup and FTM model are shown in **Fig. 10**.

The height (t_{eff}) of the truss was the center distance between the top and bottom of the hollow block.

Several methods can be used to analyze the FTM, such as the consistent deformation method, matrix method, finite element method, or FE software. Here, we analyzed the FTM structure using FE software using material properties taken from the literature as input data. The results of this validation are presented in **Fig. 11**. The FTM results compared with the three experimental specimen results are explained in the Discussion section.

3.4 Validation 3

The third validation of the FTM was conducted for low-quality brick considered by Anil *et al.* [21]. The brick had a strength of 2.5 MPa, hollow ratio of 65%, and dimensions of 185 mm × 185 mm × 135 mm. The mortar was of higher strength (5.2–7.1 MPa). The dimensions of the masonry walls were 1,600 mm × 1,100 mm × 135 mm. CFRP was coated on the side adjacent to the load side to retrofit the walls. The properties of the CFRP are given in **Table 3**. The test setup is presented in **Fig. 12.**

The CFRP was used in diverse arrays with different anchor arrangements and different combinations of vertical, horizontal, and diagonal arrangements. The CFRP arrangements were applied to 11 samples. Five sample results obtained using the FTM in this validation were satisfactory, as presented in **Fig. 13**. The results are close to the experimental values.

4. Discussion

The use of FTM to analyze a confined masonry wall under out-of-plane loading was convincing in the first validation. The maximum pressure generated by the FTM (i.e., the strength of the wall) is given in **Fig. 9.** W_t and W_c are the pressures required to produce forces on the tension truss and compression truss, respectively, that cause the wall to fail. Experimental results obtained by Varela-Rivera *et al.* [9] and displayed in **Fig. 9** revealed that specimens with similar aspect and slenderness ratios (E-1 and E-2; E-4 and E-5) have a lower out-of-plane strength than specimens with lower in-plane stiffness (E-1 and E-4). In the case of specimens with similar aspect ratios and in-plane stiffness (E-2 and E-3; E-5 and E-6), W_e is greater for specimens with smaller slenderness ratios (E-2 and E-5). The difference is related to the greater axial compressive strength of the block. The same behavior is seen in the above results obtained using the FTM. In contrast, the yield-line method and failure-line method underestimate W_e.

The FTM provides the strength resulting from a compression crack W_c and the strength resulting from a tension crack W_t . W_c represents the value of the strength resulting from an experimental crack W_e (E-2, E-3, E-4 and E-5); W_e is similar to W_c. The strength of masonry using W_{cs} (the compressive strut method) and W_{ss} (the spring-strut-method) overestimated W_e; this comparison is similar to that for W_t and W_c obtained in FTM analysis. These results are consistent with the effects of the slenderness ratio of a masonry structure in that the thickness of the masonry structure affects the pressure needed for the structure to fail. W_t and W_c were slightly greater than W_{yl} and W_e.

The FTM provided a value close to the experimental result (W_e) and the result of the spring–strut method (W_{ss}). However, W_c was a greater than W_e while W_t was lower than W_e for specimen E-1 owing to the difference in the rigidity of confinement. The rigidity of confinement depends on the reinforcement factor; this will be considered in the next FTM study.

W_t appears almost identical to W_{yl} and W_{fl}. This indicates that the previous method of obtaining W_{yl} and W_{fl} can only be used at one stage of cracking. The previous method can be applied only to a confined masonry wall. The above comparison reveals that FTM is useful in analyzing the strength of confined masonry walls.

The percentage of error (PoE) comparison between FTM and experimental and analysis results can be seen in Table 5. It is shown that for W_e (E-1) relative to FTM (W_t), PoE values are 3.9-12.1%; for E-2, E-4, and E-5 relative to W_c, PoE values are 1.9-20.9%; for W_{yl} relative to W_t, PoE values are 0.7-21.8%; for W_{fl} (E-2, E-4, E-5 end E-6) relative to W_t, the PoE values are 1.2-14.2%; for W_{ss} (E-4 and E-6) relative to W_c, PoE values are 3.3%, 7.4%, and 28.6%, and only W_{cs} relative to W_t or W_c have PoE values greater than 30%." From these results it is seen that the first crack of a masonry structure can be caused by tensile stress or compressive stress.

In the second validation, FRP was used to provide tension on the truss element. Results obtained with FTM show that the addition of FRP strengthens masonry structures, which is in line with the results of experiments. The FRP would fail before cracking appears in the area of compression [29]. The FTM reveals that the tensile load does not reach a maximum and that there is cracking as a result of compressive strain.

Figure 11 and **Table 6** shows that cracking, as a result of the truss tension obtained with the FTM, is similar to the experimental result. The percentage of error in this validation for all comparisons was between 0.82 and 27.01%.

The addition of the FRP layer provides a peak load before cracking that is higher than that for a single layer along with an increase in the loading capacity. Similarly, the two layers reduce the deformation of the structure. Apparently, retrofitting using a single layer and retrofitting using a double layer are similar under tension of the truss element, but the double layer provides different compressive strengths for the compression of the truss element. A double layer of FRP increases structural integrity, especially when the FRP layers extend to the supports [29]. Various installations of a single layer of FRP strengthen the system only slightly.

Figure 13 and Table 7 compare the results obtained using FTM with the experimental and analytical results of Anil *et al.* [21] in the third validation experiment. The FTM was used in cases with and without CFRP.

The diagonal modeling of CFRP in this validation is not applicable because the diagonal combination of CFRP strips is not handled in the two-dimensional FTM; it could be applied in three-dimensional FTM. Therefore, only certain reinforcements are used in this case, namely the reinforcements of samples 1, 8, 9, 10, and 11.

Sample 1 did not use CFRP and cracked at low load in sample 10. FTM values overestimated the load capacities compared with experimental values. For sample numbers 8, 9, and 11, FTM underestimated the load capacity results found by analysis. The average overestimation of samples 1 and 10 were around 4.27% (FTMDD) and 13.98% (FTMSD) of the load capacity values, and the average underestimation of samples 8, 9, and 11 were between 0.07% (FTMSD) and 13..98% (FTMSD) of the load capacity values. The load capacity then increased as CFRP was applied and the truss element was compressed. FTM provided results similar to the experimental results, although there were slight differences owing to the modeling of the anchor in the FTM models. The analysis of Anil *et al.* [21] overestimated the results obtained using FTM and the results obtained in experiments. Anil *et al.* did not record an analysis of sample 1.

5. Conclusions

FTM was applied to a wide variety of planar masonry structures, both confined and unconfined as well as both with and without reinforcement. The structures corresponded to a simple beam, cantilever, distributed load, and concentrated load. The following conclusions are drawn from the results of validation tests on FTM.

- FTM can be applied to various conditions of masonry structure models subject to out-of-plane loading. Specifically, FTM can be applied to a structure having an aspect ratio less than 1.
- FTM produces satisfactory results if the reinforcement of the masonry structure is uniform in direction and runs parallel to the span of the structure. However, diagonal reinforcement is difficult to model using FTM.
- FTM overcomes problems faced by previous methods because it reproduces compression and tension failures.

FTM is expected to serve as a tool for evaluating the strength of a masonry wall under out-of-plane loading. The FTM's effectiveness in three-dimensional modeling of walls will be investigated further in future work. The FTM will thus be of use to both academics and practitioners.

The symbol list

A_n	effective area n of element truss
A_c	pressure effective area
A_r	reinforcement effective area
AR	aspect ratio
A_t	tension effective area
a	depth of the equivalent stress block
α'	constants representing contribution of bricks compressive strengths on f_m
α	shape factor of compressive area
b_{eff}	width of unit load to be used
β'	constants representing contribution of mortar compressive strengths on f_m
β_1	function of strength class of materials
c	distance from center of thickness of masonry wall to the top
d_t	diagonal truss element
δ	displacement
E	Young's modulus
E_b	modulus of elasticity of bricks
E_m	modulus of elasticity of masonry
E_j	modulus of elasticity of mortar
ε'_m	peak strain in masonry, i.e., compressive strain corresponding to fm _
ε_m	compressive strain in masonry
ε	strain
E_c	modulus of elasticity of concrete
f_j	compressive strength of mortar
f'_m	compressive prism strength of masonry
f_m	compressive strength of mortar
f_b	compressive strength of brick
f_c	compressive strength of concrete
f'_{me}	compressive strength of member of truss
f_{tpe}	average out-of-plane flexural tensile strength perpendicular
f_p	compressive strength of unit masonry
FTM	fictitious truss method
FTMSD	fictitious truss method single diagonal
FTMDD	fictitious truss method double diagonal
H	height of masonry wall
h_t	horizontal truss element
I_{eq}	inertia unit equivalent of masonry element
I_n	inertia of element n equivalent of masonry element
I_{tot}	inertia unit of masonry element
θ_d	angle of diagonal truss
σu	ultimate stress
L	length of masonry wall
n	total number of data points
P	joint load
p	joint load
P_{eq}	joint load equivalent
PoE	percentage of error
Q	uniform load
t_{eff}	effective width of a cross section of truss model
v_t	vertical truss
t	thickness of masonry
t_w	thickness of masonry
$\gamma_{eq(u)}$	specific gravity equivalent of unit
$\gamma_{eq(m)}$	specific gravity equivalent of mortar
ξ	specific gravity factor
γ_u	specific gravity factor unit
γ_m	specific gravity factor mortar
γ_{eq}	specific gravity equivalent
t_w	total height of vertical truss elements
v_t	vertical truss element
W_e	strength of masonry by using experimental method
W_{ss}	strength of masonry by using spring–strut method
W_{yl}	strength of masonry by using yield-line method
W_{fl}	strength of masonry by using failure-line method
W_{cs}	strength of masonry by using compressive strut method
W_t	strength of masonry by using FTM in tension
W_c	strength of masonry by using FTM in compression
y	distance from center of effective width of a cross section of the masonry wall to center of element top truss area

References

[1] S. Noor-E-Khuda, M. Dhanasekar, and D. Thambiratnam. An explicit finite element modelling method for masonry walls under out-of-plane loading. Eng. Struct. 113 (2016) 103–120.

[2] J. Gilstrap and C. Dolan. Out-of-plane bending of FRP-reinforced masonry walls. Compos. Sci. 58(8) (1998) 1277–1284.

[3] X. Zhang, S. Singh, D. Bull, and N. Cooke. Out-of-Plane Performance of Reinforced Masonry Walls with Openings. J. Struct. Eng.-ASCE 127(1) (2001) 51–57.

[4] R. Drysdale and A. Essawy. Out-of-Plane Bending of Concrete Block Walls. J. Struct. Eng.-ASCE 114(1) (1988) 121–133.

[5] M. Griffith, J. Vaculik, Out-of-plane flexural strength of unreinforced clay brick masonry walls, TMS J. (2007).

[6] D. Abrams, R. Angel, and J. Uzarski. Out-of-Plane Strength of Unreinforced Masonry Infill Panels. Earthq. Spectra 12(4) (1996) 825–844.

[7] R. Henderson, K. Fricke, W. Jones, J. Beavers, and R. Bennett. Summary of a Large and Small-Scale Unreinforced Masonry Infill Test Program. J. Struct. Eng.-ASCE 129(12) (2003) 1667–1675.

[8] Y. Tu, T. Chuang, P. Liu, and Y. Yang. Out-of-plane shaking table tests on unreinforced masonry panels in RC frames. Eng. Struct. 32(12) (2010) 3925–3935.

[9] J. Varela-Rivera, D. Navarrete-Macias, L. Fernandez-Baqueiro, and E. Moreno. Out-of-plane behaviour of confined masonry walls. Eng. Struct. 33(5) (2011) 1734–1741.

[10] J. Varela-Rivera, J. Moreno-Herrera, I. Lopez-Gutierrez, and L. Fernandez-Baqueiro. Out-of-Plane Strength of Confined Masonry Walls. J. Struct. Eng.-ASCE 138(11) (2012) 1331–1341.

[11] J. Varela-Rivera, M. Polanco-May, L. Fernandez-Baqueiro, and E. Moreno. Confined masonry walls subjected to combined axial loads and out-of-plane uniform pressures. Can. J. Civil Eng. 39(4) (2012) 439–447.

[12] J. Moreno-Herrera, J. Varela-Rivera, and L. Fernandez-Baqueiro. Out-of-Plane Design Procedure for Confined Masonry Walls. J. Struct. Eng.-ASCE 142(2) (2016) 04015126.

[13] J. Dawe and C. Seah. Out-of-plane resistance of concrete masonry infilled panels. Can. J. Civil Eng. 16(6) (1989) 854–864.

[14] P. Agnihotri, V. Singhal, and D. Rai. Effect of in-plane damage on out-of-plane strength of unreinforced masonry walls. Eng. Struct. 57 (2013) 1–11.

[15] L. La Mendola, M. Accardi, C. Cucchiara, and V. Licata. Nonlinear FE analysis of out-of-plane behaviour of masonry walls with and without CFRP reinforcement. Constr. Build. Mater. 54 (2014) 190–196.

[16] G. Milani, M. Pizzolato, and A. Tralli. Simple numerical model with second order effects for out-of-plane loaded masonry walls. Eng. Struct. 48 (2013) 98–120.

[17] P. Asteris, L. Cavaleri, F. Di Trapani, and A. Tsaris. Numerical modelling of out-of-plane response of infilled frames: State of the art and future challenges for the equivalent strut macromodels. Eng. Struct. 132 (2017) 110–122.

[18] L. Cavaleri, M. Fossetti, and M. Papia. Modeling of Out-of-Plane Behavior of Masonry Walls. J. Struct. Eng.-ASCE 135(12) (2009) 1522–1532.

[19] D. Dizhur, M. Griffith, and J. Ingham. Out-of-plane strengthening of unreinforced masonry walls using near surface mounted fibre reinforced polymer strips. Eng. Struct. 59 (2014) 330–343.

[20] C. Willis, R. Seracino, and M. Griffith. Out-of-plane strength of brick masonry retrofitted with horizontal NSM CFRP strips. Eng. Struct. 32(2) (2010) 547–555.

[21] Ö. Anil, M. Tatayoğlu, and M. Demirhan. Out-of-plane behavior of unreinforced masonry brick walls strengthened with CFRP strips. Constr. Build. Mater. 35 (2012) 614–624.

[22] N. Ismail and J. Ingham. In-plane and out-of-plane testing of unreinforced masonry walls strengthened using polymer textile reinforced mortar. Eng. Struct. 118 (2016) 167–177.

[23] A. Furtado, H. Rodrigues, A. Arêde, and H. Varum. Experimental evaluation of out-of-plane capacity of masonry infill walls. Eng. Struct. 111 (2016) 48–63.

[24] Y. Lu and M. Panagiotou. Three-Dimensional Cyclic Beam-Truss Model for Nonplanar Reinforced Concrete Walls. J. Struct. Eng.-ASCE 140(3) (2014) 04013071.

[25] M. Moharrami, I. Koutromanos, and M. Panagiotou. Nonlinear Truss Modeling Method for the Analysis of Shear Failures in Reinforced Concrete and Masonry Structures. Improving the Seismic Performance of Existing Buildings and Other Structures (2015) 74–85.

[26] J. Almeida, P. Lourenco, and J. Barros. Characterization of brick and brick-mortar interface under uniaxial tension. VII International Seminar on Structural Masonry for Developing Countries (2002).

[27] H. Kaushik, D. Rai, and S. Jain. Stress-Strain Characteristics of Clay Brick Masonry under Uniaxial Compression. J. Mater. Civ. Eng. 19(9) (2007) 728–739.

[28] CEN 1999. Eurocode 6: Design of masonry structures- Part-1-1: General rules for reinforced and unreinforced masonry structures. European Committee for Standardization, 1 (2005) 125.

[29] S. Hamoush, M. McGinley, P. Mlakar, and M. Terro. Out-of-plane behavior of surface-reinforced masonry walls. Constr. Build. Mater. 16(6) (2002) 341–351.

[30] K. Martini. "Finite Element Studies in the Out-Of-Plane Failure of Unreinfored Masonry" Proc., 7th Int. Conf. on computing in Civil and Building Engineering, C. K. Choi, ed., Korea (1997) 179–184.

[31] SAP2000, Version 17.3.0 Build 1158. Structural Analysis Program. Berkeley, (CA), Computer and Structure, Inc. (2015).

[32] Standart Nasional Indonesia SNI 03-2847-2013. Persyaratan Beton Struktural untuk Bangunan Gedung. Badan Standarisasi Nasional (BSN), Jakarta, 2013.

[33] J. Dawe, C. Seah Out-of-plane resistance of concrete masonry infilled panels. Canadian Journal of Civil Engineering. 1989;16(6):854-864

Table captions

Table 1. Methods of analyzing masonry structures under out-of-plane loading

Table 2. Geometry, aspect ratio, and slenderness ratio of wall specimens

Table 3. Properties of SikaWrap 230-C (unidirectional) CFRP and Sikadur 330 resin

Table 4. Comparison of FTM with Varela Rivera's experimental results and various analysis methods

Table 5. Percentage of error of FTM method relative to Varela Rivera's experiment and analysis method results

Table 6. Comparison of FTM relative to Hamoush's experiment

Table 7. Comparison of FTM to Anil' experiment and analysis results

Table 1. Methods of analyzing masonry structures under out-of-plane loading

Analysis Method		Reference.
Yield line method	unreinforced wall	[4],[30]
	reinforced wall	[3]
	confined wall	[9-11]
The failure line method	unreinforced wall	[4]
	unconfined wall	[9-11]
The modified yielding line method	surrounded by steel frame	Dawe and Seah [33] cited from [12]
The compressive strut method	confined wall	[9-10]
	infill walls	[6]
The spring-strut and the bidirectional strut method	confined walls	[9-12]

Table 2. Geometry, aspect ratio, and slenderness ratio of wall specimens

Wall specimen	f_c (MPa)	f_j (MPa)	f_p (MPa)	f_m (MPa)	f_{tpe} (MPa)	f_{tpa} (MPa)	E_c (MPa)	Length L (m)	Height H (m)	Thickness t (m)	H/L	H/t
E-1	14.79	2.89	5.47	2.84	0.14	0.44	9,614	3.67	2.72	0.15	0.74	18.13
E-2	19.16	2.34	5.47	2.84	0.14	0.44	10,943	3.77	2.88	0.15	0.76	19.20
E-3	19.80	2.47	4.09	2.45	0.11	0.36	11,124	3.77	2.88	0.12	0.76	24.00
E-4	15.31	2.79	5.47	2.84	0.14	0.44	9,782	2.85	2.72	0.15	0.95	18.13
E-5	17.39	2.66	5.47	2.84	0.14	0.44	10,425	2.95	2.72	0.15	0.92	18.13
E-6	21.67	2.26	4.09	2.45	0.11	0.36	11,638	2.95	2.72	0.12	0.92	22.67

Data taken from Varela-Rivera *et al.* [9]

Table 3. Properties of SikaWrap 230-C (unidirectional) CFRP and Sikadur 330 resin

Properties of CFRP	Remarks of CFRP
Thickness (mm)	0.12
Tensile strength (MPa)	4100
Elastic modulus (MPa)	231,000
Ultimate tensile strain (%)	1.7%
Properties of resin	Remarks of resin
Tensile strength (MPa)	30
Elastic modulus (MPa)	3800

(Data taken from Anil *et al*. [21])

Table 4. Comparison of FTM with Varela Rivera's experimental results and various analysis methods

Wall specimen (kPa)		E-1	E-2	E-3	E-4	E-5	E-6
W_e (Varela Rivera experiment)		8.79	13.01	12.01	14.53	17.83	15.40
W_{yl} (Yield line method)		7.01	7.18	3.74	9.31	9.35	4.89
W_{fl} (Failure line method)		6.21	6.33	3.30	8.71	8.75	4.57
W_{cs} (Compressive strut method)		38.55	38.55	17.33	33.21	33.21	14.93
W_{ss} (Spring strut method)		6.57	30.42	11.91	15.39	30.08	11.54
Double Diagonal	W_t (FTMDD)	9.85	7.23	4.56	9.51	9.00	4.44
	δ. (mm)	13.22	14.89	18.72	12.82	12.26	15.07
	W_c (FTMDD)	14.76	11.46	8.05	14.26	13.48	8.03
	δ. (mm)	19.81	23.60	33.08	19.21	18.37	27.30
Single Diagonal	W_t (FTMSD)	9.13	6.78	4.40	8.82	8.38	4.27
	δ. (mm)	12.67	14.29	17.08	12.28	11.81	14.88
	W_c (FTMSD)	15.42	11.94	8.30	14.89	14.09	8.24
	δ. (mm)	21.40	25.15	32.27	20.74	19.85	28.73

Table 5. Percentage of error of FTM method relative to Varela Rivera's experiment and analysis method results

Wall specimen (kPa)	E-1	E-2	E-3	E-4	E-5	E-6
We (Varela Rivera experiment)	8.79	13.01	12.01	14.53	17.83	15.40
Wt (FTMDD)	9.85	7.23	4.56	9.51	9.00	4.44
% of error	**12.06**	44.41	62.06	34.53	49.53	71.20
Wt (FTMSD)	9.13	6.78	4.40	8.82	8.38	4.27
% of error	**3.85**	47.88	63.40	39.33	52.98	72.27
Wc (FTMDD)	14.76	11.46	8.05	14.26	13.48	8.03
% of error	67.95	**11.88**	32.95	**1.88**	**24.38**	47.83
Wc (FTMSD)	15.42	11.94	8.30	14.89	14.09	8.24
% of error	75.4	**8.3**	30.9	**2.5**	**20.9**	46.5

Yield line method

Wall specimen	E-1	E-2	E-3	E-4	E-5	E-6
Wyl (Yield line method)	7.01	7.18	3.74	9.31	9.35	4.89
Wt (FTMDD)	9.85	7.23	4.56	9.51	9.00	4.44
% of error	40.52	**0.72**	**21.83**	**2.18**	**3.76**	**9.29**
Wt (FTMSD)	9.13	6.78	4.40	8.82	8.38	4.27
% of error	30.22	**5.56**	**17.54**	**5.31**	**10.33**	**12.69**
Wc (FTMDD)	14.76	11.46	8.05	14.26	13.48	8.03
% of error	110.60	59.67	115.33	53.13	44.20	64.30
Wc (FTMSD)	15.42	11.94	8.30	14.89	14.09	8.24
% of error	119.95	66.23	122.06	59.92	50.75	68.52

Failure line method

Wall specimen	E-1	E-2	E-3	E-4	E-5	E-6
Wfl (Failure line method)	6.21	6.33	3.30	8.71	8.75	4.57
Wt (FTMDD)	9.85	7.23	4.56	9.51	9.00	4.44
% of error	58.62	**14.25**	38.08	**9.22**	**2.84**	**2.94**
Wt (FTMSD)	9.13	6.78	4.40	8.82	8.38	4.27
% of error	47.00	**7.13**	33.21	**1.22**	**4.18**	**6.57**
Wc (FTMDD)	14.76	11.46	8.05	14.26	13.48	8.03
% of error	137.73	81.11	144.04	63.68	54.09	75.80
Wc (FTMSD)	15.42	11.94	8.30	14.89	14.09	8.24
% of error	148.28	88.55	151.66	70.94	61.08	80.32

Compressive strut method

Wall specimen	E-1	E-2	E-3	E-4	E-5	E-6
Wcs (Compressive strut method)	38.55	38.55	17.33	33.21	33.21	14.93

Wt (FTM DD)	9.85	7.23	4.56	9.51	9.00	4.44
% of error	74.4	81.2	73.7	71.4	72.9	70.3
Wt (FTM SD)	9.13	6.78	4.40	8.82	8.38	4.27
% of error	76.3	82.4	74.6	73.5	74.8	71.4
Wc (FTM DD)	14.76	11.46	8.05	14.26	13.48	8.03
% of error	61.7	70.3	53.5	57.1	59.4	46.2
Wc (FTM SD)	15.42	11.94	8.30	14.89	14.09	8.24
% of error	60.0	69.0	52.1	55.2	57.6	44.8

Spring strut method

Wall specimen	E-1	E-2	E-3	E-4	E-5	E-6
Wss (Spring strut method)	6.57	30.42	11.91	15.39	30.08	11.54
Wt (FTM DD)	9.85	7.23	4.56	9.51	9.00	4.44
% of error	49.93	76.23	61.74	38.19	70.08	61.56
Wt (FTM SD)	9.13	6.78	4.40	8.82	8.38	4.27
% of error	38.95	77.71	63.09	42.72	72.13	63.00
Wc (FTM DD)	14.76	11.46	8.05	14.26	13.48	8.03
% of error	124.70	62.31	32.38	**7.37**	55.18	30.38
Wc (FTM SD)	15.42	11.94	8.30	14.89	14.09	8.24
% of error	134.68	60.76	30.27	**3.26**	53.14	**28.59**

Table 6. Comparison of FTM relative to Hamoush's experiment

	Distance of fiber to support											
	2L-d/4		2L-d/2		2L-0		1L-d/4		1L-0		1L-d/2	
	Max. load kN	δ. mm	Max. load kN	δ. mm	Max. load kN	δ. mm	Max. load kN	δ. mm	Max. load kN	δ. mm	Max. load kN	δ. mm
Spec.1	65.84	2.47	49.84	3.33	41.23	2.69	47.17	2.87	45.14	4.05	51.6	2.75
Spec.2	51.17	2.10	55.95	2.71	46.49	3.22	49.80	3.76	56.41	2.60	57.97	3.23
Spec.3	40.21	1.75	52.59	4.49	53.69	3.53	48.99	3.25	49.94	3.05	47.58	2.76
Average	52.41	2.11	52.79	3.51	47.14	3.15	48.65	3.29	50.50	3.23	52.38	2.91
FTMSD	59.93	3.17	60.00	3.38	59.87	3.34	59.93	3.17	59.96	5.36	60.00	5.48
% of error	14.35	50.43	13.65	3.62	27.01	6.13	23.17	3.77	18.75	65.71	14.55	88.08
FTMDD	53.53	2.62	53.43	2.63	53.13	2.63	49.06	3.67	48.93	3.69	48.81	3.72
% of error	2.15	24.15	1.21	25.20	12.72	16.50	0.83	11.42	3.10	14.22	6.82	27.84

Table 7. Comparison of FTM to Anil' experiment and analysis results

	Anil's-1		Anil's-8		Anil's-9		Anil's-10		Anil's-11	
	Load kN	δ. mm	Load kN	δ. mm	Load kN	δ. mm	Load kN	δ. mm	Load kN	δ. mm
Anil's experiment	1.76	0.91	16.47	8.14	14.50	5.83	11.74	7.10	19.71	10.93
Anil's Analysis	-		25.28		25.28		20.51		20.51	
FTMSD	2.16	3.72	16.48	24.56	16.71	23.32	10.10	20.77	17.70	33.15
% of error	22.67		0.07		15.22		13.98		10.18	
FTMDD	1.84	3.58	16.28	29.05	16.86	22.66	9.60	22.75	16.14	31.19
% of error	4.27		1.16		16.28		18.21		18.09	

46

Figure captions

Figure 1. Establishing truss blocks and configuring the truss structure.

Figure 2. Truss shapes.

Figure 3. Determination of the effective height of a truss element.

Figure 4. Equivalent inertia of the effective cross section.

Figure 5. Schematic of the proposed FTM.

Figure 6. Stress–strain relationship of truss elements representing masonry walls

Figure 7. Setup of air bag (source Herrera *et al.* [12])

Figure 8. FTM model for Varela Rivera's setup

Figure 9. Comparison of results for the first validation experiment

Figure 10. Hamoush's test setup and FTM model.

Figure 11. Comparison of results for the second validation experiment.

Figure 12. Anil's test setup and FTM model

Figure 13. Comparison of results for the third validation experiment.

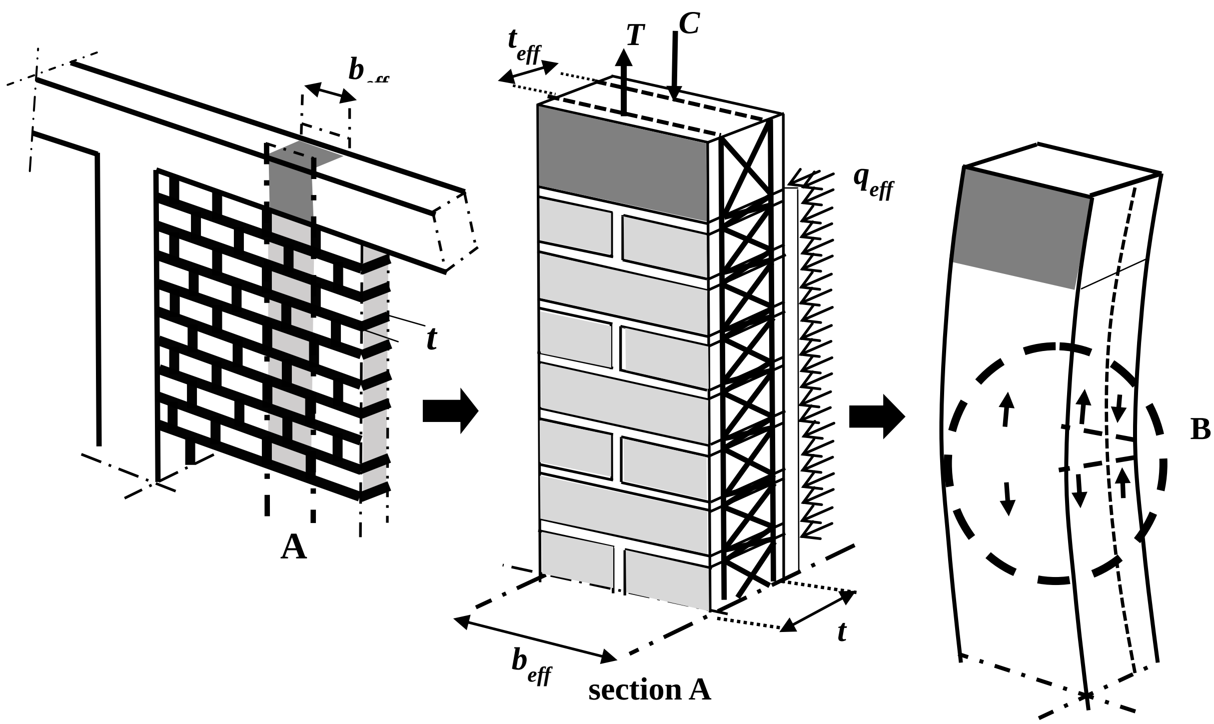

Figure 1. Establishing truss blocks and configuring the truss structure.

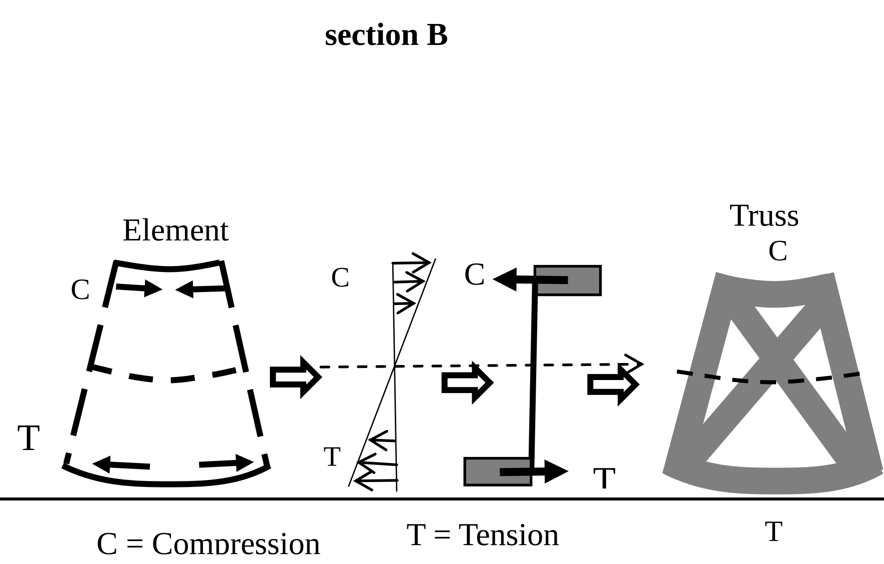

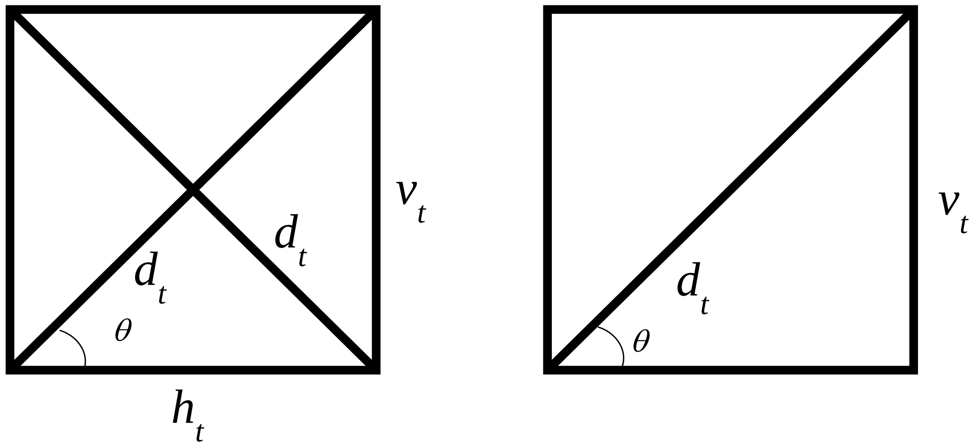

Figure 2. Truss shapes.

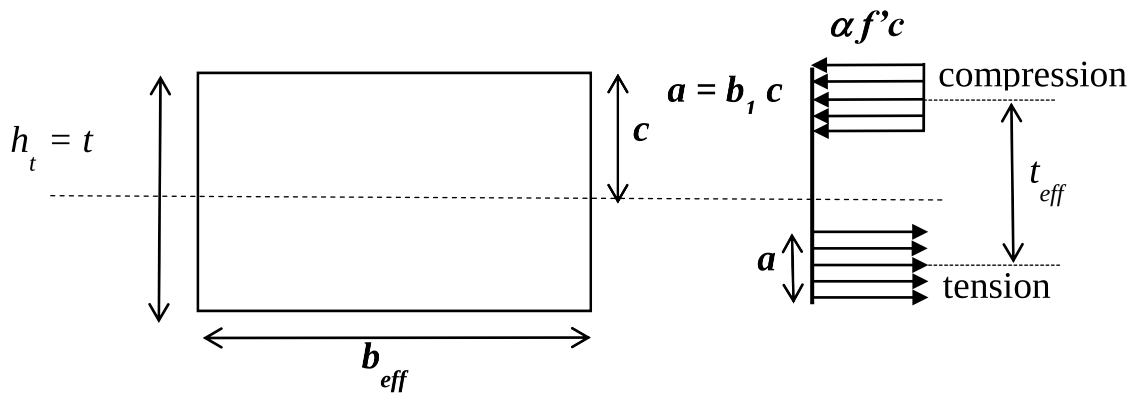

Figure 3. Determination of the effective height of a truss element.

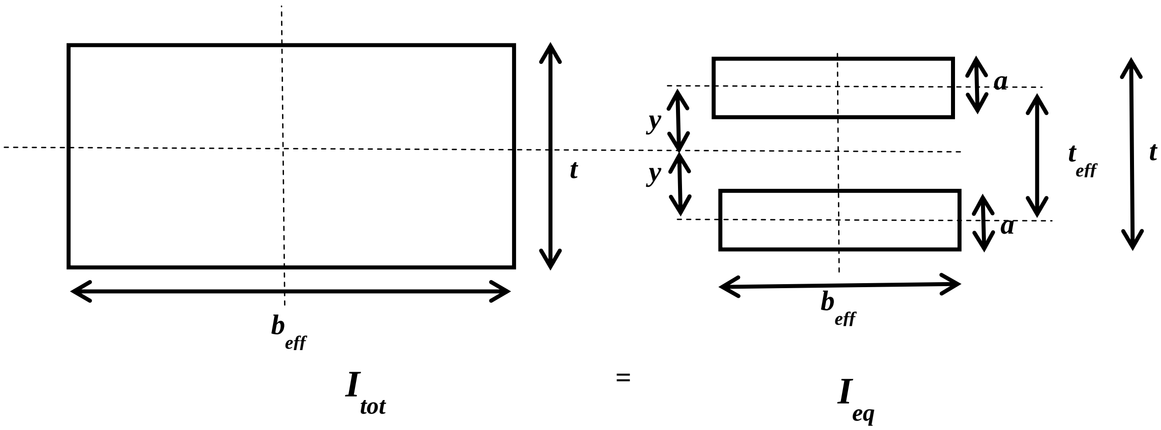

Figure 4. Equivalent inertia of the effective cross section.

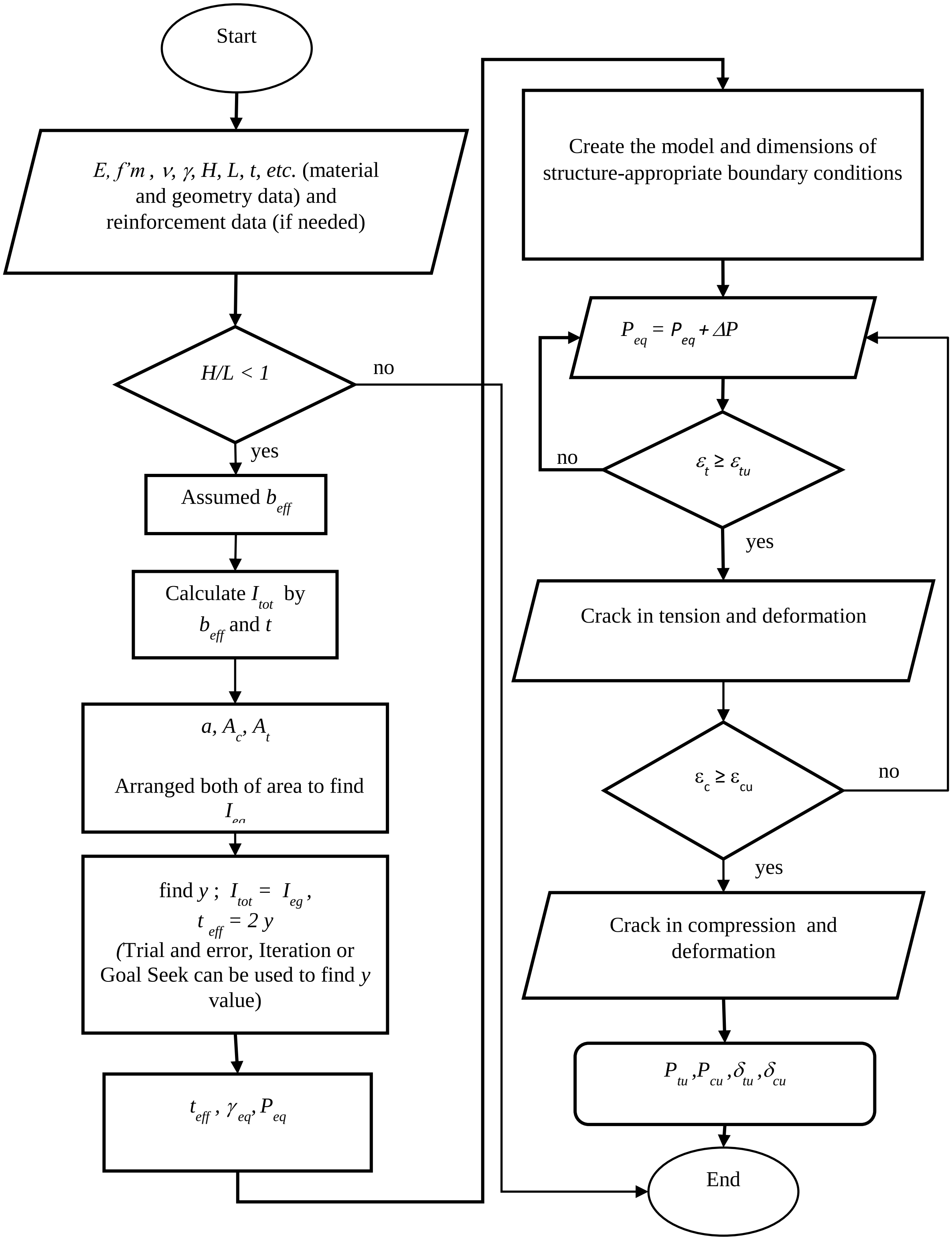
Start
E, f'm , ν, γ, H, L, t, etc. (material and geometry data) and reinforcement data (if needed)
H/L < 1
no
yes
Assumed b_{eff}
Calculate I_{tot} by b_{eff} and t
a, A_c, A_t
Arranged both of area to find I_{eq}
find y ; I_{tot} = I_{eg} , t_{eff} = 2 y
(Trial and error, Iteration or Goal Seek can be used to find y value)
t_{eff} , γ_{eq}, P_{eq}
Create the model and dimensions of structure-appropriate boundary conditions
$P_{eq} = P_{eq} + \Delta P$
$\varepsilon_t \geq \varepsilon_{tu}$
no
yes
Crack in tension and deformation
$\varepsilon_c \geq \varepsilon_{cu}$
no
yes
Crack in compression and deformation
P_{tu} ,P_{cu} ,δ_{tu} ,δ_{cu}
End

Figure 5. Schematic of the proposed FTM.

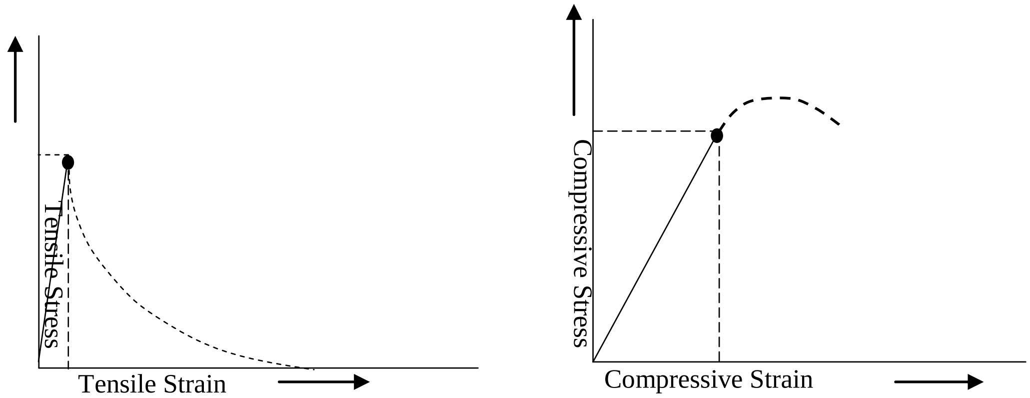

Figure 6. Stress–strain relationship of truss elements representing masonry walls

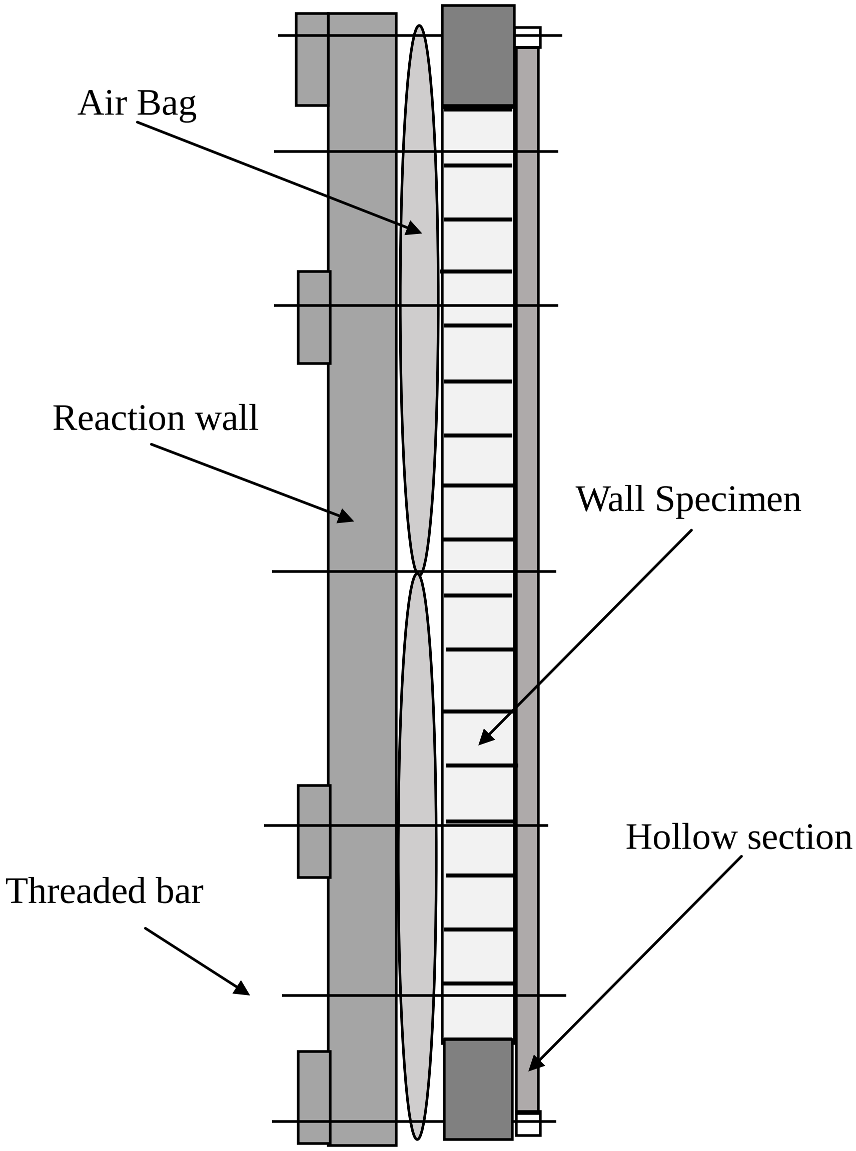

Figure 7. Setup of air bag (source Herrera *et al.* [12])

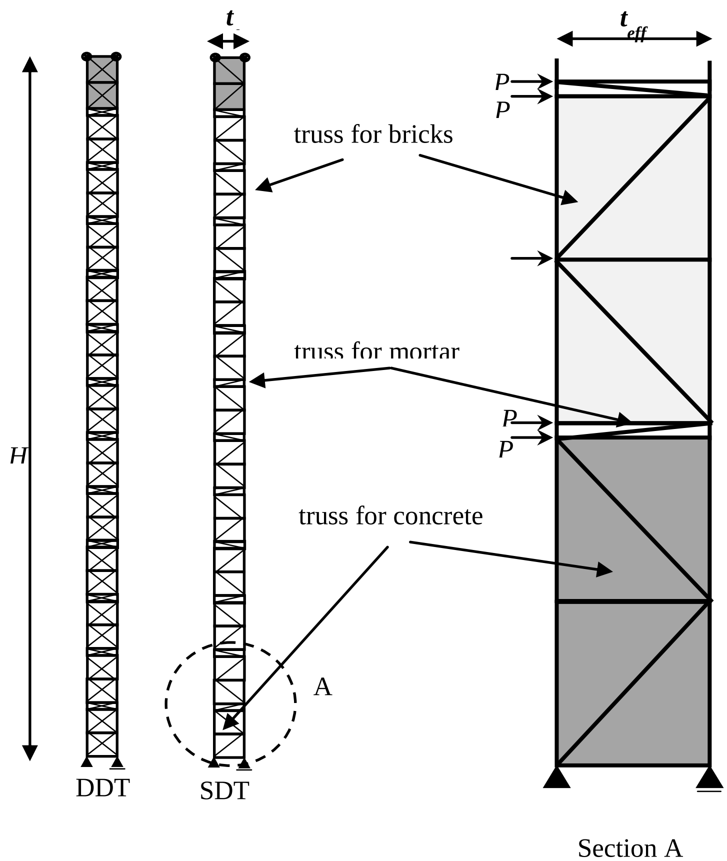

	t mm	b_{eff} mm	a mm	y mm	t_{eff} mm
E1	150	200	63.75	43.21	86.42
E2	150	200	63.75	43.21	86.42
E3	120	200	51.00	34.57	69.14
E4	150	200	63.75	43.21	86.42
E5	150	200	63.75	43.21	86.42
E6	120	200	51.00	34.57	69.14

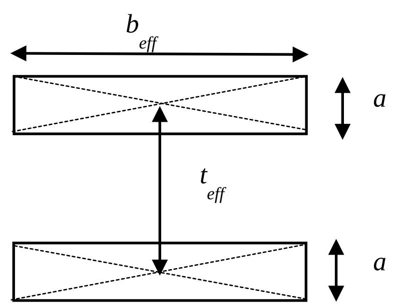

Figure 8. FTM model for Varela Rivera's setup

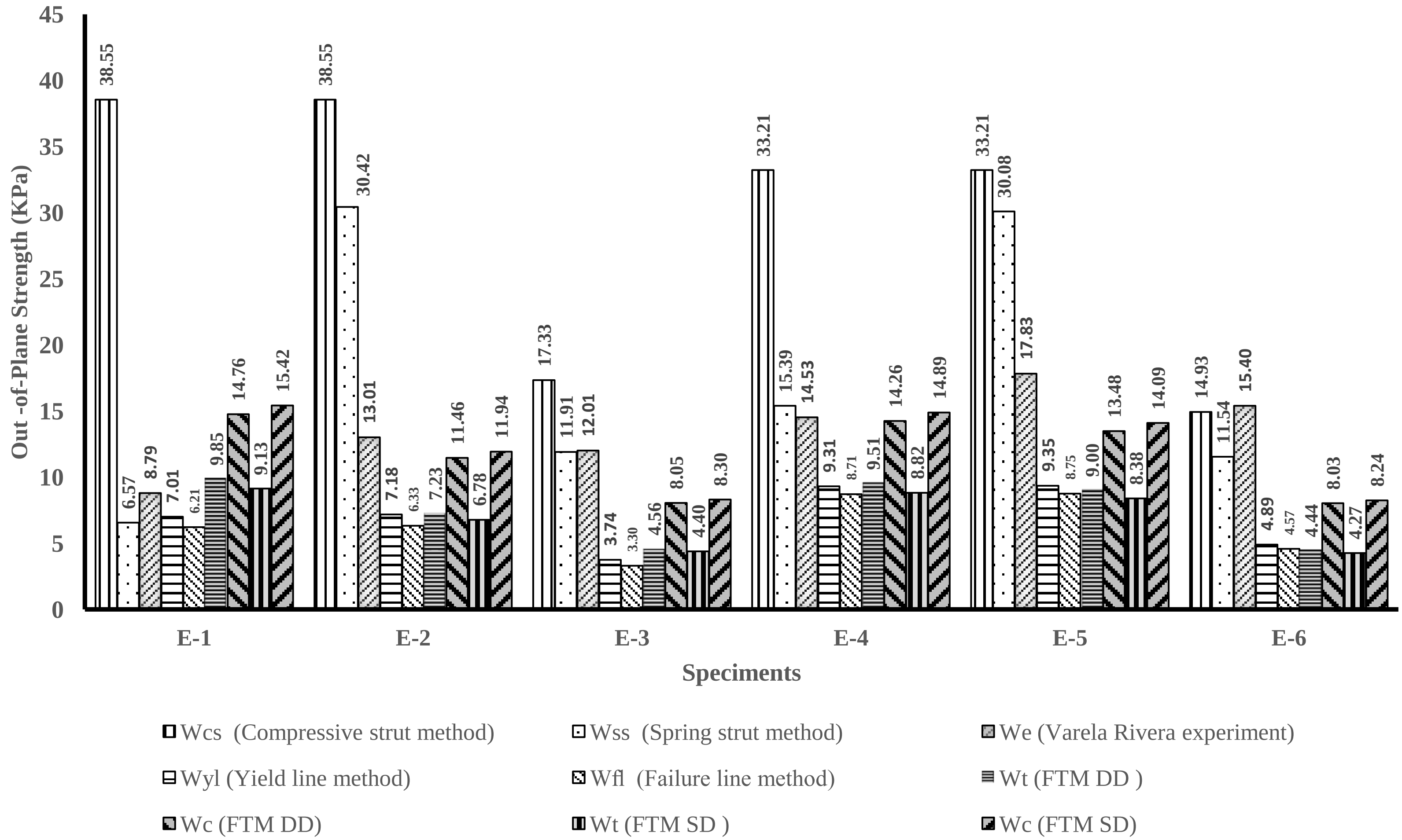

53 **Figure 9.** Comparison of results for the first validation experiment

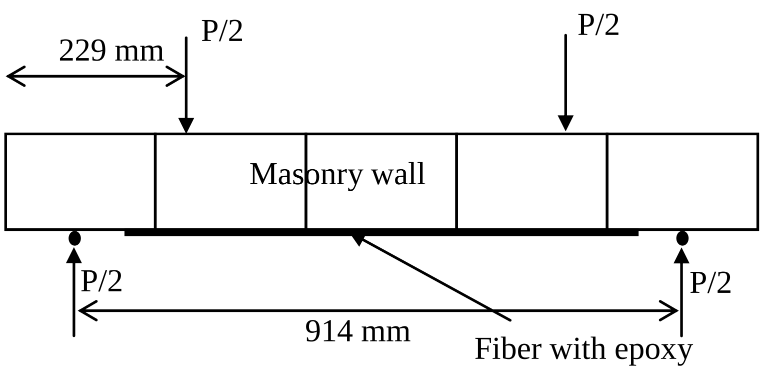

a. Hamoush test setup

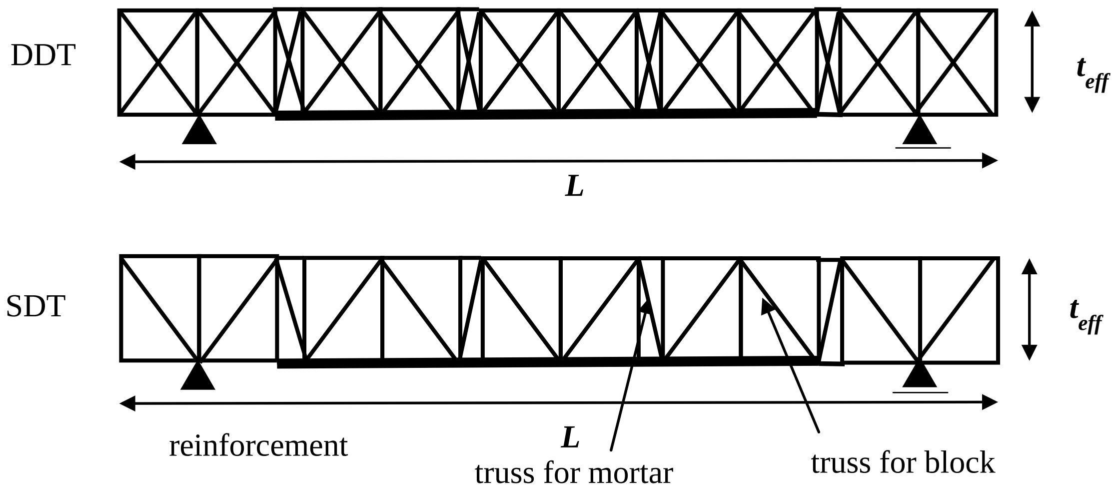

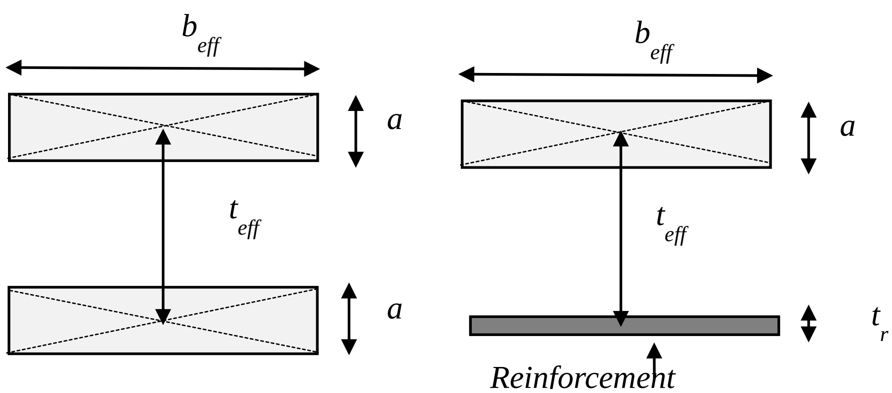

L (mm)	H (mm)	t (mm)	b_{eff} (mm)	a (mm)	y (mm)	t_{eff} (mm)
600	900	200	200	85.00	38.89	77.78

b. FTM model

Figure 10. Hamoush's test setup and FTM model.

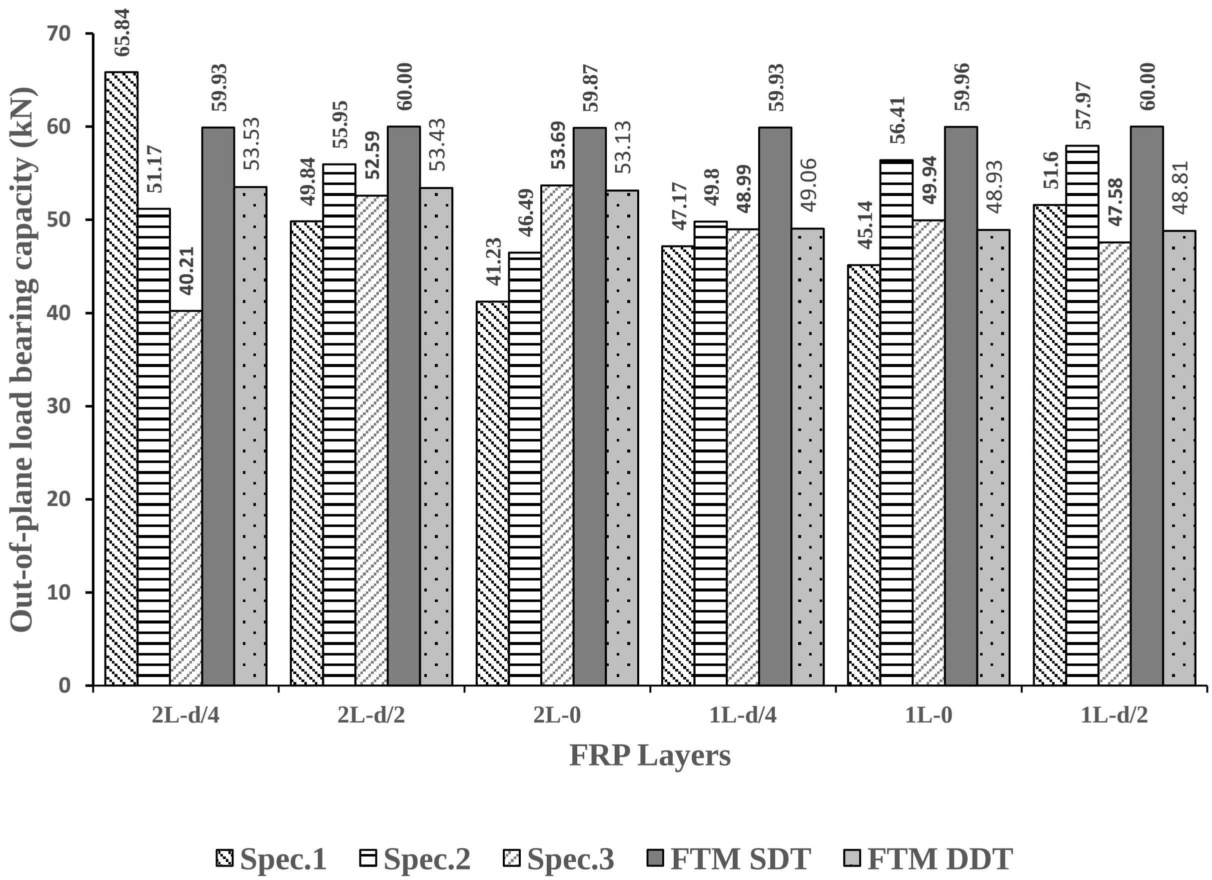

Figure 11. Comparison of results for the second validation experiment.

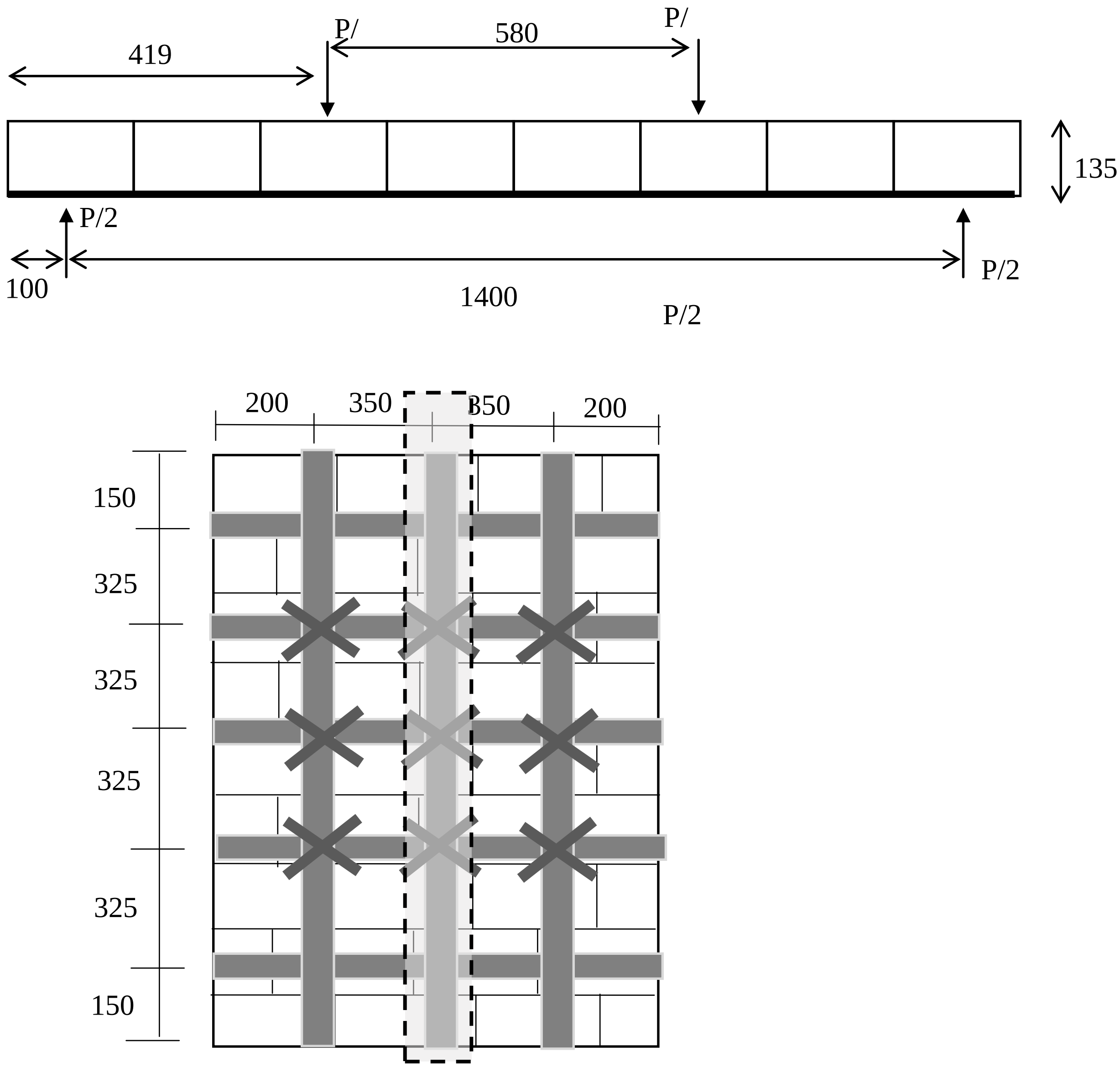

Speciment 11

a. Anil's test setup

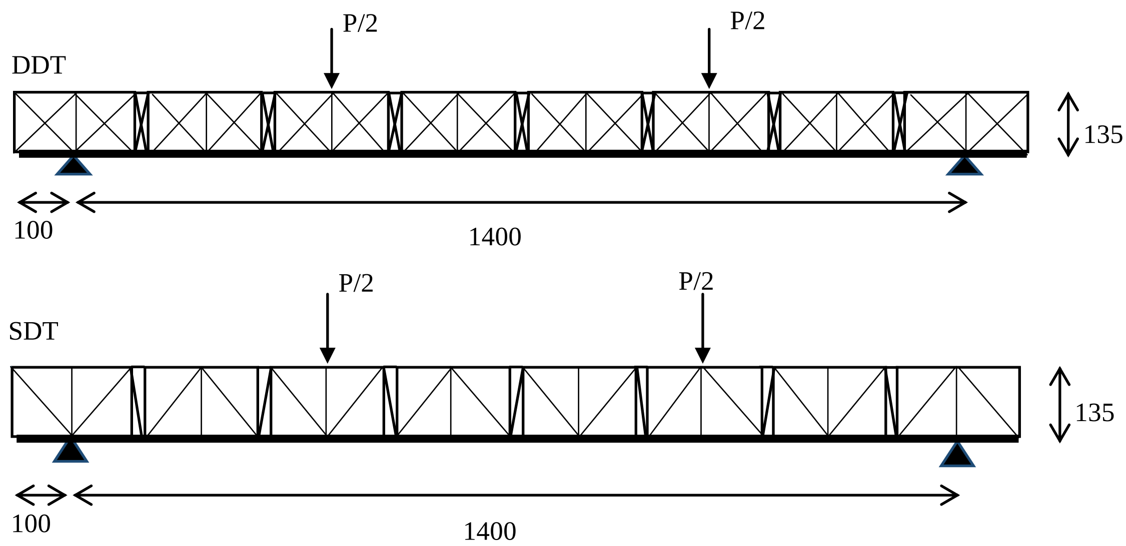

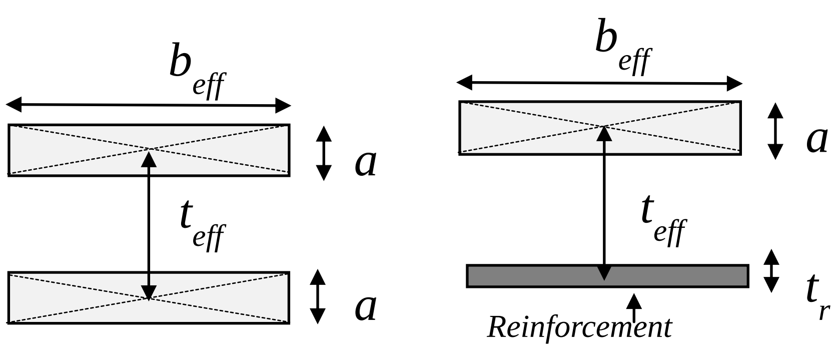

L (mm)	*H* (mm)	*t* (mm)	b_{eff} (mm)	*a* (mm)	*y* (mm)	t_{eff} (mm)
1100	1600	135	185	37.29	52.50	105.00

b. FTM model

Figure 12. Anil's test setup and FTM model..

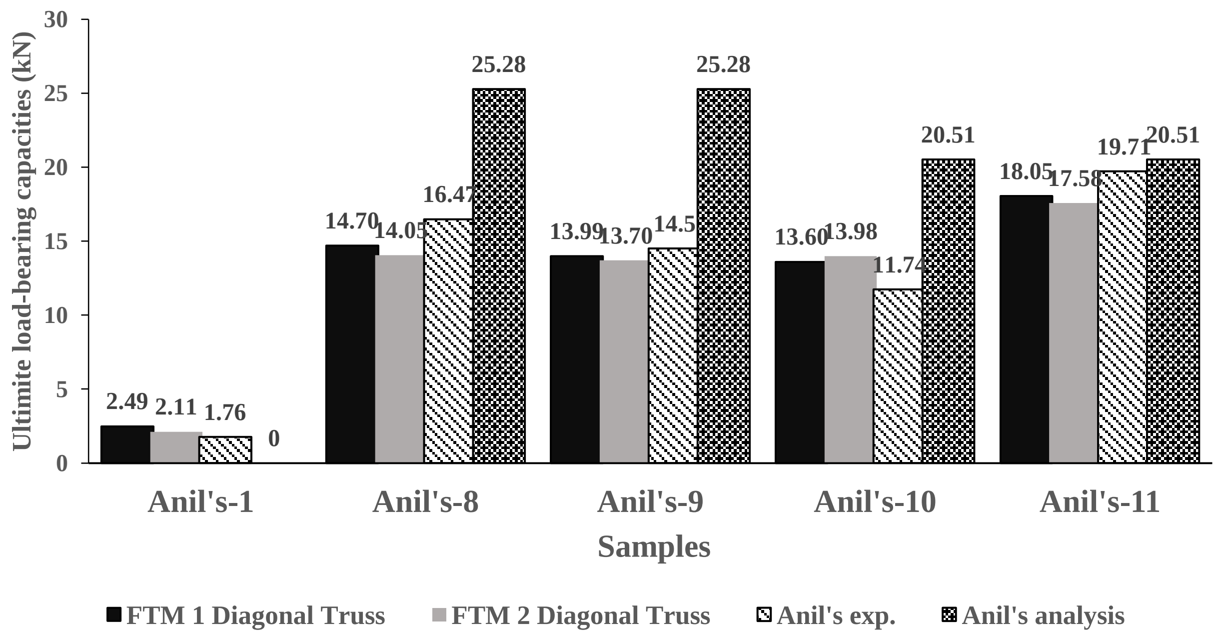

Figure 13. Comparison of results for the third validation experiment.